Published in final edited form as:
Neurobiol Dis. 2010 March ; 37(3): 711–722. doi:10.1016/j.nbd.2009.12.010.

Ethyl pyruvate protects against hypoxic-ischemic brain injury via anti-cell death and anti-inflammatory mechanisms

Hongxia Shen[1], **Xiaoming Hu**[2,3], **Can Liu**[1], **Suping Wang**[2,3], **Wenting Zhang**[1], **Hui Gao**[1], **R. Anne Stetler**[2,3], **Yanqin Gao**[*,1,2], and **Jun Chen**[*,1,2,3]

[1]State Key Laboratory of Medical Neurobiology and Institute of Brain Sciences, Fudan University, Shanghai 200032, China

[2]Department of Neurology, University of Pittsburgh School of Medicine, Pittsburgh, Pennsylvania 15213, USA

[3]Geriatric Research, Educational and Clinical Center Veterans Affairs, Pittsburgh Health Care System, Pittsburgh, Pennsylvania 15260, USA

Abstract

Ethyl pyruvate (EP) is protective in experimental models of many illnesses. This study investigates whether EP can protect against neonatal hypoxic-ischemic (H-I) brain injury. Pre-treatment with EP significantly reduced brain damage at 7 days post-H-I, with 50 mg/kg EP achieving over 50% recovery in tissue loss compared to vehicle-treated animals. Delayed treatment with EP until 30 min after H-I was still neuroprotective. EP-afforded brain protection, together with neurological function improvement, was observed up to 2 months after H-I. We further demonstrated an inhibitory effect of EP on cell death, both in an *in vivo* model of H-I and in *in vitro* neuronal cultures subjected to OGD, by reducing calpain activation and calcium dysregulation. Moreover, EP exerted an anti-inflammatory effect in microglia by inhibiting NF-κB activation and subsequent release of inflammatory mediators. Taken together, our results suggest that EP confers potent neuroprotection against neonatal H-I brain injury via its anti-cell death and anti-inflammatory actions. EP is a potential novel therapeutic agent for neonatal H-I brain injury.

Keywords

neonatal hypoxia-ischemia; neuroprotection; cell death; inflammation; microglia; calpain; calcium; NF-κB

INTRODUCTION

Perinatal hypoxic-ischemic (H-I) brain injury is a common cause of neurological deficits in children (Chang and Huang, 2006). The mechanisms of H-I-induced brain damage are heterogeneous. A complex series of pathological events including apoptosis, inflammation, oxidative stress and excitotoxicity after H-I injury are known to precipitate neuronal demise

*Corresponding authors: Dr. Jun Chen, Department of Neurology, S-507, Biomedical Science Tower, University of Pittsburgh School of Medicine, Pittsburgh, PA 15213, USA, chenj2@upmc.edu, or Dr. Yanqin Gao, State Key Laboratory of Medical Neurobiology, Fudan University School of Medicine, Shanghai 200032, China, yqgao@shmu.edu.cn.

and subsequent neurological dysfunction (Benjelloun et al., 1999; Blomgren and Hagberg, 2006; Johnston, 2005; Northington et al., 2001). H-I lesion to the brain has been shown to result in earlier acute necrotic neuronal death in the core of the infarction, followed by a delayed but prolonged apoptotic-like neuronal death in the surrounding zone (Nakajima et al., 2000; Northington et al., 2001). A rapidly expanding body of evidence also indicates that cerebral inflammation, characterized by activation of microglia and macrophages, leukocyte infiltration, release of pro-inflammatory cytokines, and increased expression of endothelial adhesion molecules (Barone and Feuerstein, 1999; del Zoppo et al., 2000), also contributes substantially to the pathogenesis of perinatal H-I brain injury (Benjelloun et al., 1999). The synergistic actions of these pathological processes exacerbate brain injury, leading to deterioration of neurological functions (Barone and Feuerstein, 1999). Therefore, therapeutic strategies that can target multiple mechanisms could be extremely useful in limiting post-H-I neuronal damage.

Ethyl pyruvate (EP) is a stable lipophilic ester derivative of pyruvate. EP was initially reported to ameliorate structural and functional damage associated with mesenteric ischemia and reperfusion in rats (Sims et al., 2001). Subsequent *in vivo* studies documented therapeutic benefits of EP in experimental models of many illnesses, such as coronary ischemia and reperfusion injury (Woo et al., 2004), hemorrhagic shock (Tawadrous et al., 2002; Yang et al., 2002), severe sepsis (Ulloa et al., 2002; Zhang et al., 2009), and acute pancreatitis (Yang et al., 2004b; Yang et al., 2008). The neuroprotective effect of EP was also observed in post-ischemic brain using an adult rat model of middle cerebral artery occlusion (MCAO) (Kim et al., 2005; Yu et al., 2005). The effect of EP in immature brain after H-I, however, is unknown. Multiple mechanisms such as metabolic augmentation, inflammatory response suppression and radical scavenging have been suggested to be involved in the protective effect of EP (Kim et al., 2008; Tokumaru et al., 2009). However, the specific molecular target of EP that produces neuroprotection remains to be elucidated.

In the current study, we explored the protective effect of EP in neonatal brain after H-I injury and investigated the molecular mechanisms underlying the action of EP. Using a rat model of neonatal H-I brain injury that induces considerable unilateral damage in cortical, hippocampal and striatal regions, we found that intraperitoneal injections of EP resulted in marked and prolonged neuroprotection. We further demonstrated that EP protects against H-I via dual mechanisms. On one hand, EP directly protects neurons against H-I by inhibiting calpain activation and subsequent pro-death pathways. On the other hand, EP offers indirect neuroprotection via suppression of microglial-mediated inflammatory response.

METHODS

Rat model of H–I injury and EP administration

All animal protocols used in this study were approved by the Institutional Animal Care and Use Committee. Animals were treated humanely and with regard for alleviating suffering. Housing and breeding of animals were done in accordance with National Institutes of Health guidelines. The procedures for the modeling of neonatal H-I injury were based on the modification of the Levine method using Sprague–Dawley rat litters at postnatal day 7 (P7) (Levine, 1960; Rice et al., 1981). Pups were anesthetized with 3% isoflurane mixed with ambient air under spontaneous inhalation, and the left common carotid artery was ligated. After a 1.5-hr recovery period, the pups were placed in glass chambers containing a humidified atmosphere of 7.8% oxygen with a balance of 92.2% nitrogen, and were then submerged in a 37°C water bath to maintain normothermia. After 2.5 hr of hypoxia, the pups were returned to their dam for the indicated times (Fig. 1A). For control measurements, a sham group was included that had a ligature placed in the identical fashion but without actually occluding the vessel and without undergoing hypoxia. EP (Sigma, St. Louis, MO) was dissolved in

physiological saline for intraperitoneal administration into rats. The vehicle group received the same volume of saline intraperitoneally.

Assessment of brain damage

At 1 or 8 weeks after H-I, pups were sacrificed by decapitation, and the brains were removed and quickly frozen in isopentane cooled by dry ice. Brains were cut into 30-μm thick coronal sections and mounted on slides. Sections through the corpus callosum and dorsal hippocampus were stained with cresyl violet. The extent of tissue damage was determined by calculating the amount of surviving tissue in each section (Lubics et al., 2005). Briefly, the volume of each brain region was calculated using digitally captured images, and the percent volume loss in the lesioned versus the unlesioned hemisphere was determined for each animal using the following equation: ((volume of unlesioned hemisphere - volume of lesioned hemisphere) / volume of unlesioned hemisphere) ×100%.

Behavioral tests

Animals were subjected to behavioral assessment 2–8 weeks after H-I using the grid walking test (Lubics et al., 2005). Rats were placed on a stainless steel grid floor (20 cm × 40 cm with a mesh size of 4 cm^2) elevated 50 cm above the floor. For a 1 min observation period, the total numbers of forelimb and hindlimb steps were counted.

Embryonic neuronal culture and induction of in vitro ischemia

Embryonic cortical neuronal cultures were prepared from 17-day-old Sprague–Dawley rat embryos as previously described (Cao et al., 2002; Nagayama et al., 1999). To simulate ischemic injury, cultures were submitted to oxygen–glucose deprivation (OGD) (Cao et al., 2002). In brief, two-thirds of the culture medium was replaced four times with serum- and glucose-free medium, resulting in a final glucose concentration of less than 1 mM. The glucose-deprived neurons were then placed in a Billups-Rothenberg modular chamber (Del Mar, San Diego, CA), which was flushed for 5 min with 95% argon and 5% CO_2 to deplete O_2 and then sealed. The chamber was placed in an incubator at 37°C for 60 min and then returned to 95% air, 5% CO_2, and normal glucose medium for the time period indicated in each experiment.

Microglial cell line

The microglial HAPI cell line is a gift from Dr. James R. Connor (Hershey Medical Center, Hershey, PA). The HAPI cell is derived from rat primary microglia-enriched cultures and retains the phenotypic and morphological characteristics of microglia.

Lactate dehydrogenase (LDH) assay

Cell death was quantified by measuring LDH release from damaged cells into the culture medium (Cao et al., 2003). In brief, 10 μl aliquot of medium taken from the cell culture wells was added to 200 μl of LDH reagent (Sigma, St. Louis, MO). The emission was measured at 340 nm using a spectrophotometer plate reader.

Hoechst 33258 nuclear staining

Hoechst staining was used to measure cell death. The percentages of cells showing chromatin condensation were quantified by counting at least 3000 cells under each experimental condition (three randomly selected fields per well, four to six wells per condition per experiment, and three independent experiments).

Measurement of intracellular ROS

The production of intracellular ROS was measured by 2', 7'-dichlorofluorescin diacetate (DCFDA) oxidation 45 min after LPS treatment. Microglia cultures were seeded in 96-well plates and then exposed to 20 μM DCFDA for 1 hr, followed by pre-treatment with EP for 1 hr and treatment with HBSS containing LPS. After incubation, the fluorescence was read at 485 nm excitation and 530 nm emission on a fluorescence plate reader.

Nitrite assay

As an indicator of nitric oxide production, the amount of nitrite accumulated in culture supernatant was determined with a colorimetric assay using Griess reagent (1% sulfanilamide, 2.5% H_3PO_4, 0.1% N-(1-naphthyl) ethylenediamine dihydrochloride). Equal volumes of culture supernatant and Griess reagent were mixed and incubated for 10 min at room temperature in the dark. The absorbance at 540 nm was determined with the SpectraMax Plus microplate spectrophotometer. The concentration of nitrite in samples was determined from a sodium nitrite standard curve.

Real-time RT-PCR

Total RNA was isolated from frozen cortical samples using the RNeasy Mini Kit according to the manufacturer's instructions (Qiagen, Valencia, CA), and 5 μg was used to synthesize the first strand of cDNA using random hexamer primers and the Superscript First-Strand Synthesis System for RT-PCR (Invitrogen, Carlsbad, CA). PCR was performed using SYBR green PCR Master Mix (Applied Biosystems, Foster City, CA). The forward and reverse primers of COX-2 were GTGTCCCTTTGCCTCTTTCAAT and GAGGCACTTGCGTTGATGGT, respectively. The forward and reverse primers of IL-1α were AAGACAAGCCTGTGTTGCTGAAGG and TCCCAGAAGAAAATGAGGTCGGTC, respectively. The forward and reverse primers of IL-1β were CACCTCTCAAGCAGAGCACAG and GGGTTCCATGGTGAAGTCAAC, respectively. The forward and reverse primers of IL-6 were TCCTACCCCAACTTCCAATGCTC and TTGGATGGTCTTGGTCCTTAGCC, respectively. The forward and reverse primers of iNOS were GTGCTAATGCGGAAGGTCATG and GCTTCCGACTTTCCTGTCTCAGTA, respectively. The forward and reverse primers of GAPDH were CCAGCCTCGTCTCATAGACA and GTAACCAGGCGTCCGATACG, respectively. The forward and reverse primers of TNF-α were AAATGGGCTCCCTCTCATCAGTTC and TCTGCTTGGTGGTTTGCTACGAC, respectively. The cycle time (Ct) values of the interested genes were first normalized with GAPDH of the same sample, and then the gene expression level in vehicle- and EP-treated groups were calculated and expressed as fold change versus sham (setting sham as 1).

Proteomic-array analysis

Proteomic-array analysis was conducted using the ChemiArray™ Rat Antibody Arrays kit (Chemicon, Temecula, CA) according to the manufacturer's instructions. Signal intensity was quantified by densitometry using MCID. For each spot, the net gray level density was determined by subtracting the background gray levels from the total raw levels. A positive control was used to normalize the results from different membranes. The relative fold-difference in cytokine amount was determined in reference to the amount present on the control membrane.

Nuclear and cytosolic extracts and western blots

Nuclear and cytosolic protein extraction and western blot were done according to our previously published protocols (Cao et al., 2002). The primary antibodies used in this study were as follows: anti- NF-κB/P65, anti-histone (Santa Cruz Biotechnology, Santa Cruz, CA),

anti-active caspase-3, anti-phospho-Akt (Ser473), anti-total Akt, anti-COX-2 (Cell Signaling Technology, Danvers, MA), and anti-AIF antibody (Epitomics, Burlingame, CA).

Calpain activity assay

Calpain activity assay was performed using a fluorescent calpain I substrate as described previously (Vosler et al., 2009). In brief, mitochondrial proteins (30 μg) were incubated with calpain reaction buffer (20 mM HEPES, pH 7.6; 1 mM EDTA; 50 mM NaCl; and 0.1% (v/v) 2-mercaptoethanol) containing 10 μM calpain I fluorescent substrate H-E(EDANS)PLFAERK (DABCYL)-OH (Calbiochem, La Jolla, CA). The reaction was initiated by addition of $CaCl_2$ (final concentration of 5 μM) and incubated at 37 °C for 30 min. The activity of calpain was measured by detecting the increase in fluorescence using excitation/emission wavelengths of 335/500 nm. Calpain activity was calculated quantitatively based on the standard curve generated using recombinant calpain I (Calbiochem, La Jolla, CA) and expressed as units per milligram of protein.

Cytosolic Ca^{2+} $[Ca^{2+}]_i$ measurement

Neurons grown on coverslips were incubated with 5 μM fura-2 AM in HEPES-MEM for 30 min at 37°C. Cells were then placed in a heated open-bath imaging chamber at 37°C. Using a Nikon TE 300 inverted epifluorescence microscope and a 40x oil-immersion objective lens, neurons were excited at 345 and 385 nm, and the emission fluorescence at 510 nm was recorded. Images were collected every 1 min during a 5 min baseline, every 1 min for the second 10 min after OGD, and every 1–5 min up to 60 min after OGD. Regions of interest were subsequently analyzed with MetaFluor image-processing software. At the end of each experiment, the cells were exposed to 1 mM $MnCl_2$ in Ca^{2+}-free HEPES-MEM and 5 μM 4-bromo A-23187 to obtain Ca^{2+}-insensitive fluorescence signals. The Ca^{2+}-insensitive fluorescence signals were subtracted and the corrected 345/385 emission ratios were converted to Ca^{2+} concentration as escribed previously (Lenart et al., 2004).

Statistical analysis

All data are reported as mean±S.E.M. Statistical significance between two groups was assessed with Student's *t* test. Statistical significance between multiple groups was performed using one- or two-way ANOVA. When ANOVA showed a significant difference, a least significant difference multiple comparisons post-hoc test was performed. A value of $p<0.05$ was considered statistically significant.

RESULTS

EP protects against brain tissue loss after neonatal H-I

To evaluate the neuroprotective effect of EP against neonatal H-I-induced brain injury, EP was administered intraperitoneally at different doses (10, 30, 50, 100, 250 and 500 mg/kg) 1 hr after the left common carotid artery occlusion (CCAO) and 30 min before hypoxia (Fig. 1A). The extent of brain damage was determined 7 days after H-I by calculating the degree of tissue loss in each section. As shown in Fig. 1B, EP at concentrations ranging from 30 to 500 mg/kg significantly attenuated post-H-I brain tissue loss. The maximal protection occurred at 50 mg/kg, which reduced the tissue loss from 43.2% in vehicle-treated H-I animals to 19.8% in EP-treated H-I animals ($p<0.01$). At 500 mg/kg, the highest concentration of EP tested, neuroprotection was submaximal and was accompanied by increased mortality. The mortality rate of the procedure was increased to 20% for the animals injected with 500 mg/kg of EP, compared to less than 3% for vehicle- or lower concentration (10–250 mg/kg) EP-injected animals.

To gain further insight into the ability of systemic EP injection to protect against H-I brain injury and to establish the most favorable time window for neuroprotection after H-I, the optimal concentration of EP (50 mg/kg) was applied at various time points (10, 30, 60 or 90 min) after the completion of H-I (Fig. 1C). Significant neuroprotection was obtained with EP administration at 10 min or 30 min after completion of H-I. EP treatment at 60 min or 90 min after completion of H-I displayed a tissue loss comparable to that of the vehicle-treated mice. The optimal post-treatment regimen of EP (50 mg/kg, 10 min post-H-I) was then used in all subsequent experiments.

We next analyzed the effect of EP on individual brain regions for tissue damage. Cresyl violet staining was used to examine the cell morphology and infarct area (Fig. 1D and Fig. 2). Normal cells with round and pale stained nuclei were seen throughout the contralateral cerebral cortex, striatum, and hippocampus. There was a marked increase in dying cells, characterized by shrunken cells with pyknotic nuclei, and large areas of tissue loss in the ipsilateral cerebral cortex, striatum, and hippocampus of H-I-injured animals with vehicle treatment. EP treatment decreased the number of dying cells, as well as the area of tissue damage. Detailed quantification of damaged areas showed that tissue loss in both the cortex (64.0%) and hippocampus (68.1%) was worse compared to that in the striatum (32.9%). EP treatment significantly attenuated brain damage in the cortex, hippocampus, and striatum, reducing the tissue loss to 21.9%, 26.1% and 16.1%, respectively (Fig. 1D and 1E). Taken together, these results reveal a potent neuroprotective effect of EP against neonatal H-I injury, with greater than 50% recovery in all of the H-I sensitive regions.

We also investigated the effect of EP on the markers of cell death. Caspase-3 is the major effector caspase in the brain, particularly in the immature brain (Blomgren et al., 2001). The activation of caspase-3, which was monitored as cleaved caspase-3 by western blot, was observed in the cortical extract at 6 hr after H-I and lasted until at least 24 hr post-injury (Supplemental Fig. 1A). EP treatment significantly inhibited caspase-3 activation as compared to vehicle-treated animals at 24 hr after H-I (Supplemental Fig. 1B and 1C). Immunoreactivity towards cleaved caspase-3 (Supplemental Fig. 1D) displayed a dramatically reduced number of caspase-3-positive cells in EP-treated brain compared to that in the vehicle-treated brain after H-I. Apoptosis-inducing factor (AIF) is a predominant mediator of the caspase-independent apoptosis pathway (Boujrad et al., 2007; Culmsee and Plesnila, 2006). The translocation of AIF from mitochondria to the nucleus is necessary for AIF-induced cell death (Cheung et al., 2006). The nuclear level of AIF was examined in the cortical extract by western blot (Supplemental Fig. 1E). H-I induced nuclear expression of AIF that was early (3 hr after H-I) and persistent (until 48 hr after H-I). EP treatment completely abolished the H-I-induced nuclear translocation of AIF at 6 hr to 48 hr post-H-I. Collectively, these results suggest that EP inhibits cell death by targeting both caspase-dependent and caspase-independent pro-death pathways.

EP improves long-term neurological outcomes after H-I injury

The locomotor activity of rats subject to H-I was assessed using the grid-walking test. Animals were placed on a raised steel grid to quantify overall ambulatory behavior (Fig. 3A and 3B). Statistical significance between multiple groups was performed using two-way ANOVA with time and treatment as the independent factors. When ANOVA showed significant differences, a least significant difference multiple comparisons post-hoc test was performed. Animals subjected to H-I showed significantly reduced forelimb and hindlimb usage in comparison with sham-operated controls at 2–8 weeks post-injury. EP treatment resulted in a profound improvement of limb usage beginning the third week after H-I, and continuing till the eighth week after H-I.

Brain sections obtained at 8 weeks after H-I were analyzed for brain tissue damage. As shown in Fig. 3C, administration of EP significantly ameliorated H-I-induced brain damage, reducing tissue loss to 23.8% ($P<0.05$ vs. vehicle controls). These results, coupled with the behavioral studies, confirmed that EP actually reduced cerebral tissue loss, rather than simply delaying cell death, and thus improved long-term neurological function after H-I injury.

EP curtails neuronal cell death after oxygen glucose deprivation

To evaluate whether EP has direct protective effects on neurons and to further elucidate the underlying mechanisms, we used a well-established *in vitro* OGD model of neuronal H-I, with primary cortical neuronal cultures. EP at various concentrations was added directly to cultures prior to 60 min of OGD. EP treatment remarkably attenuated OGD-induced cell death at 24 hr after OGD in a concentration-dependent manner (Fig. 4A and 4B). Delayed treatment with EP (10 min after reperfusion) still showed strong, albeit less effective than pre-treatment, neuroprotection against OGD, as revealed by measuring LDH release (Fig. 4C), Alamar blue fluorescence (Fig. 4D) and quantification of condensed/fragmented nuclei in Hoechst staining (Fig. 4E and 4F). At all concentrations tested (0.3 to 10 mM), EP itself did not cause cell death in control non-OGD neurons (data not shown).

EP inhibits calpain activity and calcium accumulation after OGD

Calpain is a calcium-dependent cysteine protease that has been proved to be important in regulating both caspase-dependent (Blomgren et al., 2001; Nakagawa and Yuan, 2000) and caspase-independent (Cao et al., 2007; Vosler et al., 2009) mitochondrial pro-death pathways. We investigated the effect of EP on calpain activation in neurons after OGD. As shown in Fig. 4J, calpain activity elevated from 2–24 hr after OGD. EP treatment significantly inhibited OGD-induced calpain activation. Western blot was then used to detect the breakdown products of α-fodrin, which is a substrate of calpain and caspase-3, in neurons subjected to OGD. The density of the 150-kD band increased dramatically at 2, 6, and 24 hr after OGD, whereas EP suppressed the density of this band at all time points (Fig. 4I). Previous report has shown that Western blot analsis of substrate degradation is insensitive to caspase-3 activation in current OGD model (Newcomb-Fernandez et al., 2001), which is also confirmed here by the marginal change in 120-kD band (the cleavage products of caspase-3). Therefore, the 150-kDa band, although could represent the cleavage products of both calpain and caspase-3, might be mainly from calpain activation. Collectively, these data suggest that EP reduced calpain activity after ischemic insult.

Since abnormal calcium homeostasis is common in ischemic neuronal damage and since calpain activity is strictly calcium dependent, we investigated the effect of EP on intracellular calcium concentration using fura-2 AM. OGD resulted in a gradual increase in the $[Ca^{2+}]_i$ level, which reached more than 10-fold over controls at 60 min after reperfusion (Fig. 4K). EP treatment abolished the OGD-induced increases in fura-2 AM fluorescence for at least 60 min after reperfusion, suggesting that EP can correct calcium dysregulation after ischemic injury.

Several serine/threonine protein kinases, including Akt, JNK, ERK and p38 MAPK, operate upstream of mitochondrial cell death by modulating the phosphorylation status of key elements in the cell death cascades, and these have been suggested to be important in the pathogenesis of cell death upon cerebral ischemia (Namura et al., 2001; Piao et al., 2003; Wang et al., 2004; Wick et al., 2002; Yin et al., 2007; Zhang et al., 2007). We therefore sought to explore whether the neuroprotective effect of EP could be attributed to the modulation of any one of these protein kinases. We found that OGD exposure resulted in sustained diminishment of Akt phosphorylation (p-Akt) in cortical neurons, which was reinstated by EP treatment (Fig. 4G). Pharmacological inhibition of the upstream kinase PI3-K by LY294002 inhibited EP-induced Akt augmentation (Fig. 4G), but failed to abolish the EP-afforded neuroprotection against OGD

(Fig. 4H). The *in vivo* study in H-I animals replicated these *in vitro* results. A significant decrease in p-Akt levels was observed at 24 hr after H-I, as compared with non–H-I controls. EP treatment after H-I resulted in a significant increase in cortical p-Akt. Augmentation of p-Akt in EP-treated H-I animals depends on PI3-K activity, because intracerebroventricular injection of LY294002 significantly reduced its formation (Supplemental Fig. 2A and 2B). LY294002, however, failed to block the protective effect of EP on tissue loss 7 days after H-I (Supplemental Fig. 2C). These results suggest that although the PI3-K/Akt pathway can be enhanced by EP treatment, it is not a direct target for the neuroprotective effect of EP. OGD-induced changes on ERK, p38 or JNK phosphorylation were not affected by EP (Supplemental Fig. 3).

EP inhibits the inflammatory process in the neonate brain after H-I

It was previously suggested that EP suppresses the expression of pro-inflammatory mediators in several disease models (Yang et al., 2002; Yang et al., 2003; Yang et al., 2004b). To investigate the effect of EP on H-I–induced inflammation, several inflammatory markers were measured 24 hr after H-I, when inflammatory response can be reliably detected and irreversible brain damage has yet to occur. Three experimental groups, including the sham-operated control group, an H-I group with vehicle treatment, and an H-I group with EP treatment (50 mg/kg, 10 min post H-I), were tested.

First, real-time RT-PCR was used to evaluate the effect of EP treatment on mRNA expression levels of various inflammatory mediators after H-I. Four cytokines (TNF-α, IL-1α, IL-1β and IL-6) and two other inflammatory factors (COX-2 and iNOS), were significantly up-regulated in the vehicle-treated H-I brains. EP treatment significantly attenuated the H-I-induced increases in all six of these factors (Fig. 5A). Proteomic arrays were then used to examine the protein profiles of a panel of cytokines in brain protein extracts. Consistent with the real-time RT-PCR result, protein levels of TNF-α, IL-1α, IL-1β and IL-6, as well as 6 other cytokines (LIX, MIP-1, MIP-3α, βNGF, TMP-1 and IL-10), were significantly increased after H-I, and all of them were returned to levels at or below control by EP (Fig. 5B). Protein levels of COX-2 were analyzed in whole tissue extract by western blot. As expected, H-I substantially induced COX-2 expression as early as 1 hr post-H-I, and remained elevated up to 24 hr after injury. Administration of EP inhibited the expression of COX-2 down to nearly undetectable levels from 3 hr onwards (Fig. 5C).

In view of the fact that microglia are the resident inflammatory cell type in the brain and a major source of inflammatory cytokines after brain injuries, especially at early time points, we examined the effect of EP on microglial activation by immunofluorescent staining of Iba1, a marker of microglia. Although resident microglia from sham-operated animals expressed a basal level of Iba1 (Fig. 5D-a and d), they appeared small and bore thin processes (Fig. 5D-d). Microglial activation was highly visible in the brains subjected to H-I with vehicle treatment. This was demonstrated by numerous microglia assumed a highly activated amoeboid state with an enlarged cell body, thicker cellular processes and a dramatic increase in Iba1 staining (Fig. 5D-b and e). In contrast, microglial activation was markedly ameliorated in EP-treated rats (Fig. 5D-c and f), wherein far fewer amoeboid microglia were detected (Fig. 5D-f).

EP suppresses LPS-induced activation of microglia

To verify the anti-inflammatory effect of EP on microglia and to further investigate the underlying mechanisms, we examined activation of a HAPI rat microglial cell line in the presence of EP after LPS stimulation (100 ng/ml). EP treatment at concentrations ranging from 0.5 mM to 5 mM significantly blocked LPS-stimulated production of nitric oxide (NO) (Fig. 6A) and TNF-α (Fig. 6B) in a dose-dependent manner. Under all the concentrations tested, no cell toxicity was detected by measuring LDH release (data not shown). The anti-inflammatory

effect of EP was also confirmed in an *in vivo* brain inflammation model in P7 rat. Brain inflammation was induced by intracerebroventricular injection of LPS, an established model that induces inflammation with a negligible amount of neuronal death in the cortex (Milatovic et al., 2003). EP (50 mg/kg) was administered intraperitoneally at 30 min prior to LPS (3 μg). We found that the immunoreactivity of COX-2 and iNOS appeared in the cortex of LPS-treated pups at 24 hr following LPS, whereas they were barely detectable in sham-operated animals (Supplemental Fig. 4). EP treatment before LPS clearly reduced the expression of iNOS and COX-2 in the cortex, indicating an anti-inflammatory effect of EP in the brain inflammation model.

We further investigated whether the anti-inflammatory effect of EP is associated with its anti-oxidant effect. HAPI cells were pre-treated with different concentrations of EP (0.5, 1, 2, 5, 10 mM) for 1 hr, and then exposed to LPS. First, we examined the generation of H_2O_2, a byproduct of superoxide, by a quantitative kit (Invitrogen). LPS caused significant production of H_2O_2 in microglia, and EP significantly reduced LPS-induced H_2O_2 production in a dose-dependent manner to nearly or below control level (Fig. 6C). Intracellular oxidative stress in microglia was also measured via DCFH oxidation. As shown in Fig. 6D, EP significantly reduced LPS-induced intracellular ROS production in HAPI cells.

EP inhibits NF-κB signaling pathway in microglia

NF-κB plays a pivotal role as a transcriptional activator in immune and inflammatory responses and regulates the expression of many inflammatory mediators including TNF-α, IL-1α, IL-1β, COX-2 and iNOS (Saliba and Henrot, 2001). EP-mediated inhibition of mRNA expression of these NF-κB-responsive genes suggested a possible effect of EP on NF-κB activation. To test this hypothesis, the effect of EP on LPS-induced activation of NF-κB was examined by measuring the DNA binding activity of NF-κB with a TransAM ELISA kit (Active Motif, Carlsbad, CA) in HAPI cells. As shown in Fig. 6E, EP treatment significantly inhibited LPS-induced NF-κB activation. Western blot analyses showed a significant increase in NF-κB/P65 levels in nuclear fraction from HAPI cells at 1 hr post-LPS, which was reduced in the presence of EP treatment (Fig. 6F). We also confirmed p65 translocation using immunofluorescent staining. As shown in Fig. 7G, p65 stayed mostly in the cytosol under normal condition. In response to LPS stimulation, p65 dramatically increased translocation into the nucleus. The LPS-induced p65 translocation was inhibited by EP treatment.

The inhibitory effect of EP on NF-κB signaling was confirmed in an *in vivo* neonatal H-I model. Nuclear and cytosolic extracts from cortical tissue were obtained and analyzed for p65 levels using western blot analysis (Supplemental Fig. 5). Vehicle-treated animals showed vastly increased nuclear p65 1–24 hr after H-I compared to sham-treated animals. Treatment with EP completely abolished this increase beginning 3 hr after H-I.

DISCUSSION

Neonatal H-I brain injury is an important clinical problem associated with high morbidity and mortality. Current available therapies for this disease are rather limited. In this study, we demonstrated, for the first time, that EP significantly reduced brain damage and improved neurological outcomes evaluated up to 2 months after neonatal H-I injury. Brain tissue loss was ameliorated even when EP administration was delayed for up to 30 min following the H-I insult. Further mechanistic studies identified two mechanisms that underlie the EP-afforded neuroprotection against cerebral H-I injury: one for direct neuronal protection via inhibition of cell death pathways, and the other for indirect neuroprotection via suppression of microglia-mediated inflammation.

Although EP has been reported to ameliorate organ dysfunction and/or improve survival in various animal models of human diseases (Kim et al., 2005; Sims et al., 2001; Tawadrous et al., 2002; Ulloa et al., 2002; Woo et al., 2004; Yang et al., 2008; Yu et al., 2005), very few of them showed a full range of *in vivo* dose-response profile. In this study, a concentration range from 30 mg/kg to 250 mg/kg for a single intraperitoneal injection of EP significantly protected the immature brain from H-I injury without increasing mortality rate in experimental animals. The maximal brain protection was achieved at 50 mg/kg, which is consistent with the efficacious dose (40–50 mg/kg) determined in an adult rat cerebral ischemia model of MCAO (Yu et al., 2005) and other preclinical studies in rodents. This dosage of EP has also been tested in human volunteers and has shown to be safe and well-tolerated (Fink, 2007). Increasing EP dose over 50 mg/kg offered no further protection against brain tissue loss.

While Yu et al. reported that EP afforded observable neuroprotection even when it was administered 24 hr after reperfusion in an adult ischemic model (Yu et al., 2005), a narrower temporal therapeutic window of a comparable dose of EP was observed in our study with a neonatal H-I brain injury model, where delivery of EP delayed by 30 min after H-I was efficacious but delays in treatment of 60 min or more were unable to achieve neuroprotection. This implies that EP may have to be given either before or soon after neonatal H-I in order to be of benefit. A post-insult administration regimen was used in most experiments in this study because it has greater clinical relevance than pre-insult administration of EP into uterus as a preventative measure.

Programmed cell death is known to play a more pronounced role in neonatal than in adult cerebral injury (Northington et al., 2005; Zhu et al., 2005). It might therefore be that the immature brain can benefit more from the protective effect of anti-apoptotic therapies than the adult brain. It has been suggested that both caspase-dependent (Yin et al., 2006) and caspase-independent (Zhu et al., 2007) cell death pathways are activated in damaged neurons after H-I brain injury. We demonstrated that EP treatment ameliorated caspase-dependent cell death after H-I, as revealed by inhibited activation of caspase-3 in the brain. This finding is in line with previous studies showing that EP inhibits caspase-3 activation in PC-12 cells upon dopamine exposure (Wang et al., 2005), in hepatic cells after liver ischemia/reperfusion (Tsung et al., 2005) and in hematopoietic progenitor cells (32Dcl3 cells) upon radiation (Epperly et al., 2007). An important novel finding in this study is that EP also inhibits caspase-independent apoptosis after H-I, as demonstrated by reduced nuclear translocation of AIF. These data suggest an anti-cell death property of EP via modulating multiple mitochondrial pro-death signaling pathways.

Our data in neuronal cultures confirmed the protective effect of EP in neurons after ischemic insults. Furthermore, we showed a suppressive effect of EP on calpain activity in neurons after OGD. Calpain has been proved to be important in regulating both caspase-dependent and caspase-independent mitochondrial pro-death pathways. Calpains and caspase–3 mutually regulate each other; calpain promotes activation of caspase-3 (Blomgren et al., 2001; Nakagawa and Yuan, 2000) and caspase-3 positively regulates calpain by cleaving calpastatin, the endogenous calpain inhibitor (Blomgren et al., 1999; Porn-Ares et al., 1998). It has also been demonstrated that AIF truncation and release is dependent upon calpain activation in isolated mitochondria (Polster et al., 2005), primary neurons (Vosler et al., 2009) and rat brain (Cao et al., 2007). Thus, the inhibitory effect of EP on calpain activation after OGD could result in reduced neuronal death and explain, at least in part, the neuroprotective effect of EP.

The precise mechanism by which EP modulates calpain activity is still elusive. It has been shown that EP can enhance ATP generation (Devamanoharan et al., 1999; Taylor et al., 2005). However, our data showed that EP was effective even when administrated after the completion of H-I. This post-treatment effectiveness suggests that EP may target some

processes other than or in addition to the energy restoration. One possibility from this study is that EP corrects perturbed calcium homeostasis after H-I. Calcium intracellular accumulation and massive influx into mitochondria have been reported after ischemia-induced neuronal damage (Choi, 1995; Domoki et al., 2004), which can lead to calpain activation (Vosler et al., 2009). We showed that EP successfully inhibited the intracellular calcium accumulation in neurons for at least 60 min after OGD. This will result in suppression of calcium-dependent calpain activity. In addition to affecting calpain activation, abnormal calcium homeostasis could result in increased ROS production in mitochondria (Maciel et al., 2001; Starkov et al., 2004). Mitochondrial Ca^{2+} overload subsequent to excessive intracellular Ca^{2+} also leads to the opening of the mitochondrial permeability transition pore and the release of apoptotic factors (Baumgartner et al., 2009), inducing cell death. With the ability to correct calcium homeostasis, EP may mitigate all of these detrimental events in insulted neurons and thus reduce neuronal death.

We also found that EP enhanced the activation of Akt, a neuronal survival factor that plays a critical role in balancing cell death (Yang et al., 2004a), after OGD in a PI3-K-dependent manner. However, inhibition of PI3-K/Akt did not affect EP-conferred neuroprotection. Our results indicate that, although the activation of PI3-K/Akt might be associated with the action of EP, it is not required for EP-mediated neuroprotection and thus cannot be a direct target of EP.

Of note, our *in vitro* data in neuronal cultures showed that pre-treatment with EP afforded better protection in comparison with post-treatment against OGD, while in *in vivo* studies, post-treatment and pre-treatment with EP demonstrated comparable protection against H-I. These results suggest that some post-H-I mechanisms targeting non-neuronal cells might be involved in the action of EP.

The role of inflammation is recognized to have a considerable influence in the pathogenesis of neonatal H-I brain injury (Benjelloun et al., 1999). Microglia, as a key player in neuro-inflammatory response and a major contributor to the excessive production of pro-inflammatory cytokines and other mediators, can respond promptly to H-I injury and accumulate in and around ischemic regions within 10 min post-injury (Biran et al., 2006; Cai et al., 2006; Carty et al., 2008; Hagberg et al., 1996). The EP-conferred inhibition of microglial activation and production of pro-inflammatory mediators in the H-I-affected neonatal brain indicate that microglial suppression might be another mechanism by which EP exerts its neuroprotective effect. Further study revealed that EP was capable of suppressing inflammatory response in a microglial cell line and in the P7 rat brain following LPS, a potent microglia stimulator. Taken together, these data suggest that the inflammation-suppressing effect of EP in H-I brain may be ascribed, at least in part, to its direct interference with the signaling processes governing inflammation regulation in microglia, instead of (or in addition to) a result secondary to the reduced tissue damage. This is consistent with recent work showing that EP exerts anti-inflammatory effects on macrophage-like cells *in vitro* (Han et al., 2005; Kim et al., 2008; Song et al., 2004) and in animal models of sepsis (Ulloa et al., 2002), colitis (Dave et al., 2009) and stroke (Kim et al., 2005).

The molecular basis for the anti-inflammatory effect of EP through NF-κB modulation has been reported (Han et al., 2005; Kim et al., 2008). Recent studies showed that in macrophage (Han et al., 2005) and endothelial cell (Johansson and Palmblad, 2009), EP interacts with NF-κB by directly targeting p65 subunit. Consistently, our *in vivo* studies demonstrated that EP treatment inhibited H-I-induced p65 nuclear translocation and expression of several NF-κB-responsive genes (TNF-α, IL-1α, IL-1β, COX-2 and iNOS), suggesting the involvement of such NF-κB modulation in the anti-inflammatory effect of EP following H-I. In addition, we showed strong intracellular ROS scavenging capacity of EP in microglia. ROS produced by

phagocytic cells are components of the microglial inflammatory response and important for microglia-mediated neurotoxicity (Gao et al., 2003; Qin et al., 2004). Alternatively, ROS function as second messengers to regulate downstream signaling molecules, including NF-κB (Schreck et al., 1991), amplifying the production of proinflammatory cytokines, such as TNF-α (Forman et al., 2002). Thus, the ROS scavenging property may be another potential anti-inflammatory mechanism for EP in microglia.

Previous studies have demonstrated that neuroprotection against ischemic brain injury by merely targeting one specific pathway of the ischemic cascade is incomplete (De Keyser et al., 1999; Yin et al., 2006). Treatment strategies that target multiple mechanisms are therefore important for the successful reduction of H-I brain injury. Our data demonstrate that EP confers significant neuroprotection against neonatal H-I brain injury. Both indirect (anti-inflammation) and direct (anti-cell death) mechanisms underlie the neuroprotective properties of EP. Additionally, studies *in vitro* and in other animal models have shown that EP treatment could reduce oxidative stress (Kim et al., 2008; Varma et al., 1998) and enhance ATP generation (Devamanoharan et al., 1999; Taylor et al., 2005), all of which may contribute to EP-afforded neuroprotection against H-I. With its protective potency and multiple-targeting capacity, further investigation into EP as a therapeutic agent for neonatal H-I brain injury is warranted.

Taken together, our study showed that EP protects against brain damage and improves the long-term neurological function after H-I. We further demonstrated an inhibitory effect of EP on cell death, both in an *in vivo* model of H-I and in *in vitro* neuronal cultures subjected to OGD, by reducing calpain activation and calcium dysregulation. Moreover, EP exerted an anti-inflammatory effect in microglia by inhibiting NF-κ B activation and subsequent release of inflammatory mediators. Our results suggest that EP is a potential novel therapeutic agent for neonatal H-I brain injury.

Supplementary Material

Refer to Web version on PubMed Central for supplementary material.

Acknowledgments

H.S. and X.H. contributed equally to this manuscript. This project was supported by NIH/NINDS grants NS36736, NS43802, and NS45048 (to J.C.). Y.G. was supported by the Chinese Natural Science Foundation (grants 30470592 and 30670642,and J0730860). C.L. was supported by the Chinese Natural Science Foundation (grant J0730860). We thank Carol Culver for excellent editorial assistance.

REFERENCES

Barone FC, Feuerstein GZ. Inflammatory mediators and stroke: new opportunities for novel therapeutics. J Cereb Blood Flow Metab 1999;19:819–834. [PubMed: 10458589]

Baumgartner HK, et al. Calcium Elevation in Mitochondria Is the Main Ca2+ Requirement for Mitochondrial Permeability Transition Pore (mPTP) Opening. J Biol Chem 2009;284:20796–20803. [PubMed: 19515844]

Benjelloun N, et al. Inflammatory responses in the cerebral cortex after ischemia in the P7 neonatal Rat. Stroke 1999;30:1916–1923. discussion 1923–4. [PubMed: 10471445]

Biran V, et al. Glial activation in white matter following ischemia in the neonatal P7 rat brain. Exp Neurol 2006;199:103–112. [PubMed: 16697370]

Blomgren K, Hagberg H. Free radicals, mitochondria, and hypoxia-ischemia in the developing brain. Free Radic Biol Med 2006;40:388–397. [PubMed: 16443153]

Blomgren K, et al. Calpastatin is up-regulated in response to hypoxia and is a suicide substrate to calpain after neonatal cerebral hypoxia-ischemia. J Biol Chem 1999;274:14046–14052. [PubMed: 10318818]

Blomgren K, et al. Synergistic activation of caspase-3 by m-calpain after neonatal hypoxia-ischemia: a mechanism of "pathological apoptosis"? J Biol Chem 2001;276:10191–10198. [PubMed: 11124942]

Boujrad H, et al. AIF-mediated programmed necrosis: a highly regulated way to die. Cell Cycle 2007;6:2612–2619. [PubMed: 17912035]

Cai Z, et al. Minocycline alleviates hypoxic-ischemic injury to developing oligodendrocytes in the neonatal rat brain. Neuroscience 2006;137:425–435. [PubMed: 16289838]

Cao G, et al. Translocation of apoptosis-inducing factor in vulnerable neurons after transient cerebral ischemia and in neuronal cultures after oxygen-glucose deprivation. J Cereb Blood Flow Metab 2003;23:1137–1150. [PubMed: 14526224]

Cao G, et al. In Vivo Delivery of a Bcl-xL Fusion Protein Containing the TAT Protein Transduction Domain Protects against Ischemic Brain Injury and Neuronal Apoptosis. J Neurosci 2002;22:5423–5431. [PubMed: 12097494]

Cao G, et al. Critical role of calpain I in mitochondrial release of apoptosis-inducing factor in ischemic neuronal injury. J Neurosci 2007;27:9278–9293. [PubMed: 17728442]

Carty ML, et al. Post-insult minocycline treatment attenuates hypoxia-ischemia-induced neuroinflammation and white matter injury in the neonatal rat: a comparison of two different dose regimens. Int J Dev Neurosci 2008;26:477–485. [PubMed: 18387771]

Chang YC, Huang CC. Perinatal brain injury and regulation of transcription. Curr Opin Neurol 2006;19:141–147. [PubMed: 16538087]

Cheung EC, et al. Dissociating the dual roles of apoptosis-inducing factor in maintaining mitochondrial structure and apoptosis. Embo J 2006;25:4061–4073. [PubMed: 16917506]

Choi DW. Calcium: still center-stage in hypoxic-ischemic neuronal death. Trends Neurosci 1995;18:58–60. [PubMed: 7537408]

Culmsee C, Plesnila N. Targeting Bid to prevent programmed cell death in neurons. Biochem Soc Trans 2006;34:1334–1340. [PubMed: 17073814]

Dave SH, et al. Ethyl pyruvate decreases HMGB1 release and ameliorates murine colitis. J Leukoc Biol. 2009

De Keyser J, et al. Clinical trials with neuroprotective drugs in acute ischaemic stroke: are we doing the right thing? Trends Neurosci 1999;22:535–540. [PubMed: 10542428]

del Zoppo G, et al. Inflammation and stroke: putative role for cytokines, adhesion molecules and iNOS in brain response to ischemia. Brain Pathol 2000;10:95–112. [PubMed: 10668900]

Devamanoharan PS, et al. Attenuation of sugar cataract by ethyl pyruvate. Mol Cell Biochem 1999;200:103–109. [PubMed: 10569189]

Domoki F, et al. Diazoxide prevents mitochondrial swelling and Ca2+ accumulation in CA1 pyramidal cells after cerebral ischemia in newborn pigs. Brain Res 2004;1019:97–104. [PubMed: 15306243]

Epperly M, et al. Ethyl pyruvate, a potentially effective mitigator of damage after total-body irradiation. Radiat Res 2007;168:552–559. [PubMed: 17973549]

Fink MP. Ethyl pyruvate: a novel anti-inflammatory agent. J Intern Med 2007;261:349–362. [PubMed: 17391109]

Forman HJ, et al. Redox signaling. Mol Cell Biochem 2002;234–235:49–62.

Gao HM, et al. Novel anti-inflammatory therapy for Parkinson's disease. Trends Pharmacol Sci 2003;24:395–401. [PubMed: 12915048]

Hagberg H, et al. Enhanced expression of interleukin (IL)-1 and IL-6 messenger RNA and bioactive protein after hypoxia-ischemia in neonatal rats. Pediatr Res 1996;40:603–609. [PubMed: 8888290]

Han Y, et al. Ethyl pyruvate inhibits nuclear factor-kappaB-dependent signaling by directly targeting p65. J Pharmacol Exp Ther 2005;312:1097–1105. [PubMed: 15525791]

Johansson AS, Palmblad J. Ethyl pyruvate modulates adhesive and secretory reactions in human lung epithelial cells. Life Sci 2009;84:805–809. [PubMed: 19345231]

Johnston MV. Excitotoxicity in perinatal brain injury. Brain Pathol 2005;15:234–240. [PubMed: 16196390]

Kim HS, et al. Ethyl pyruvate has an anti-inflammatory effect by inhibiting ROS-dependent STAT signaling in activated microglia. Free Radic Biol Med 2008;45:950–963. [PubMed: 18625301]

Kim JB, et al. Anti-inflammatory mechanism is involved in ethyl pyruvate-mediated efficacious neuroprotection in the postischemic brain. Brain Res 2005;1060:188–192. [PubMed: 16226231]

Lenart B, et al. Na-K-Cl cotransporter-mediated intracellular Na+ accumulation affects Ca2+ signaling in astrocytes in an in vitro ischemic model. J Neurosci 2004;24:9585–9597. [PubMed: 15509746]

Levine S. Anoxic-ischemic encephalopathy in rats. Am J Pathol 1960;36:1–17. [PubMed: 14416289]

Lubics A, et al. Neurological reflexes and early motor behavior in rats subjected to neonatal hypoxic-ischemic injury. Behav Brain Res 2005;157:157–165. [PubMed: 15617782]

Maciel EN, et al. Oxidative stress in Ca(2+)-induced membrane permeability transition in brain mitochondria. J Neurochem 2001;79:1237–1245. [PubMed: 11752064]

Milatovic D, et al. Pharmacologic suppression of neuronal oxidative damage and dendritic degeneration following direct activation of glial innate immunity in mouse cerebrum. J Neurochem 2003;87:1518–1526. [PubMed: 14713307]

Nagayama T, et al. Cannabinoids and neuroprotection in global and focal cerebral ischemia and in neuronal cultures. J Neurosci 1999;19:2987–2995. [PubMed: 10191316]

Nakagawa T, Yuan J. Cross-talk between two cysteine protease families. Activation of caspase-12 by calpain in apoptosis. J Cell Biol 2000;150:887–894. [PubMed: 10953012]

Nakajima W, et al. Apoptosis has a prolonged role in the neurodegeneration after hypoxic ischemia in the newborn rat. J Neurosci 2000;20:7994–8004. [PubMed: 11050120]

Namura S, et al. Intravenous administration of MEK inhibitor U0126 affords brain protection against forebrain ischemia and focal cerebral ischemia. Proc Natl Acad Sci U S A 2001;98:11569–11574. [PubMed: 11504919]

Newcomb-Fernandez JK, et al. Concurrent assessment of calpain and caspase-3 activation after oxygen-glucose deprivation in primary septo-hippocampal cultures. J Cereb Blood Flow Metab 2001;21:1281–1294. [PubMed: 11702043]

Northington FJ, et al. Early Neurodegeneration after Hypoxia-Ischemia in Neonatal Rat Is Necrosis while Delayed Neuronal Death Is Apoptosis. Neurobiol Dis 2001;8:207–219. [PubMed: 11300718]

Northington FJ, et al. Apoptosis in perinatal hypoxic-ischemic brain injury: how important is it and should it be inhibited? Brain Res Brain Res Rev 2005;50:244–257. [PubMed: 16216332]

Piao CS, et al. Administration of the p38 MAPK inhibitor SB203580 affords brain protection with a wide therapeutic window against focal ischemic insult. J Neurosci Res 2003;73:537–544. [PubMed: 12898538]

Polster BM, et al. Calpain I induces cleavage and release of apoptosis-inducing factor from isolated mitochondria. J Biol Chem 2005;280:6447–6454. [PubMed: 15590628]

Porn-Ares MI, et al. Cleavage of the calpain inhibitor, calpastatin, during apoptosis. Cell Death Differ 1998;5:1028–1033. [PubMed: 9894609]

Qin L, et al. NADPH oxidase mediates lipopolysaccharide-induced neurotoxicity and proinflammatory gene expression in activated microglia. J Biol Chem 2004;279:1415–1421. [PubMed: 14578353]

Rice JE 3rd, et al. The influence of immaturity on hypoxic-ischemic brain damage in the rat. Ann Neurol 1981;9:131–141. [PubMed: 7235629]

Saliba E, Henrot A. Inflammatory mediators and neonatal brain damage. Biol Neonate 2001;79:224–227. [PubMed: 11275656]

Schreck R, et al. Reactive oxygen intermediates as apparently widely used messengers in the activation of the NF-kappa B transcription factor and HIV-1. Embo J 1991;10:2247–2258. [PubMed: 2065663]

Sims CA, et al. Ringer's ethyl pyruvate solution ameliorates ischemia/reperfusion-induced intestinal mucosal injury in rats. Crit Care Med 2001;29:1513–1518. [PubMed: 11505117]

Song M, et al. Evidence that glutathione depletion is a mechanism responsible for the anti-inflammatory effects of ethyl pyruvate in cultured lipopolysaccharide-stimulated RAW 264.7 cells. J Pharmacol Exp Ther 2004;308:307–316. [PubMed: 14569076]

Starkov AA, et al. Mitochondrial calcium and oxidative stress as mediators of ischemic brain injury. Cell Calcium 2004;36:257–264. [PubMed: 15261481]

Tawadrous ZS, et al. Resuscitation from hemorrhagic shock with Ringer's ethyl pyruvate solution improves survival and ameliorates intestinal mucosal hyperpermeability in rats. Shock 2002;17:473–477. [PubMed: 12069183]

Taylor MD, et al. Ethyl pyruvate enhances ATP levels, reduces oxidative stress and preserves cardiac function in a rat model of off-pump coronary bypass. Heart Lung Circ 2005;14:25–31. [PubMed: 16352248]

Tokumaru O, et al. Neuroprotective effects of ethyl pyruvate on brain energy metabolism after ischemia-reperfusion injury: a 31P-nuclear magnetic resonance study. Neurochem Res 2009;34:775–785. [PubMed: 18985448]

Tsung A, et al. Ethyl pyruvate ameliorates liver ischemia-reperfusion injury by decreasing hepatic necrosis and apoptosis. Transplantation 2005;79:196–204. [PubMed: 15665768]

Ulloa L, et al. Ethyl pyruvate prevents lethality in mice with established lethal sepsis and systemic inflammation. Proc Natl Acad Sci U S A 2002;99:12351–12356. [PubMed: 12209006]

Varma SD, et al. Prevention of intracellular oxidative stress to lens by pyruvate and its ester. Free Radic Res 1998;28:131–135. [PubMed: 9645390]

Vosler PS, et al. Calcium dysregulation induces apoptosis-inducing factor release: Cross-talk between PARP-1- and calpain- signaling pathways. Exp Neurol 2009;218:213–220. [PubMed: 19427306]

Wang LZ, et al. Ethyl pyruvate protects PC12 cells from dopamine-induced apoptosis. Eur J Pharmacol 2005;508:57–68. [PubMed: 15680254]

Wang ZQ, et al. U0126 prevents ERK pathway phosphorylation and interleukin-1beta mRNA production after cerebral ischemia. Chin Med Sci J 2004;19:270–275. [PubMed: 15669185]

Wick A, et al. Neuroprotection by hypoxic preconditioning requires sequential activation of vascular endothelial growth factor receptor and Akt. J Neurosci 2002;22:6401–6407. [PubMed: 12151519]

Woo YJ, et al. Ethyl pyruvate preserves cardiac function and attenuates oxidative injury after prolonged myocardial ischemia. J Thorac Cardiovasc Surg 2004;127:1262–1269. [PubMed: 15115981]

Yang JY, et al. Surviving the kiss of death. Biochem Pharmacol 2004a;68:1027–1031. [PubMed: 15313397]

Yang R, et al. Ethyl pyruvate modulates inflammatory gene expression in mice subjected to hemorrhagic shock. Am J Physiol Gastrointest Liver Physiol 2002;283:G212–G221. [PubMed: 12065309]

Yang R, et al. Ethyl pyruvate ameliorates acute alcohol-induced liver injury and inflammation in mice. J Lab Clin Med 2003;142:322–331. [PubMed: 14647036]

Yang R, et al. Ethyl pyruvate ameliorates distant organ injury in a murine model of acute necrotizing pancreatitis. Crit Care Med 2004b;32:1453–1459. [PubMed: 15241088]

Yang ZY, et al. Delayed ethyl pyruvate therapy attenuates experimental severe acute pancreatitis via reduced serum high mobility group box 1 levels in rats. World J Gastroenterol 2008;14:4546–4550. [PubMed: 18680237]

Yin W, et al. TAT-mediated delivery of Bcl-xL protein is neuroprotective against neonatal hypoxic-ischemic brain injury via inhibition of caspases and AIF. Neurobiol Dis 2006;21:358–371. [PubMed: 16140540]

Yin W, et al. Preconditioning suppresses inflammation in neonatal hypoxic ischemia via Akt activation. Stroke 2007;38:1017–1024. [PubMed: 17272774]

Yu YM, et al. Inhibition of the cerebral ischemic injury by ethyl pyruvate with a wide therapeutic window. Stroke 2005;36:2238–2243. [PubMed: 16141417]

Zhang QG, et al. Critical role of PTEN in the coupling between PI3K/Akt and JNK1/2 signaling in ischemic brain injury. FEBS Lett 2007;581:495–505. [PubMed: 17239858]

Zhang Y, et al. Effect of ethyl pyruvate on physical and immunological barriers of the small intestine in a rat model of sepsis. J Trauma 2009;66:1355–1364. [PubMed: 19430239]

Zhu C, et al. Apoptosis-inducing factor is a major contributor to neuronal loss induced by neonatal cerebral hypoxia-ischemia. Cell Death Differ 2007;14:775–784. [PubMed: 17039248]

Zhu C, et al. The influence of age on apoptotic and other mechanisms of cell death after cerebral hypoxia-ischemia. Cell Death Differ 2005;12:162–176. [PubMed: 15592434]

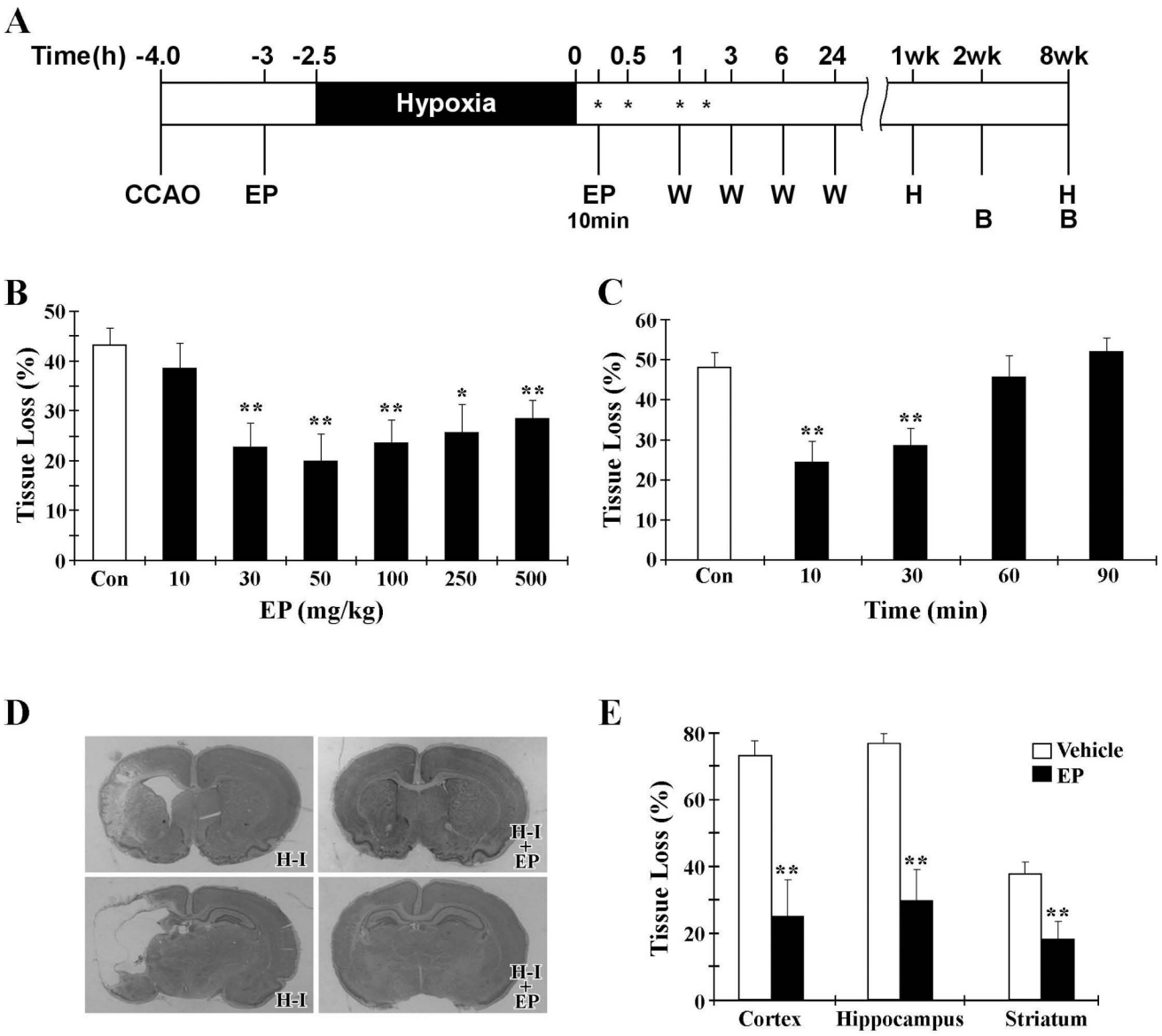

Figure 1. Protective effect of EP against H-I brain injury in neonates

A. Timeline showing the induction of H-I and the time points for various assays (hours or weeks after completion of H-I). EP was administered as a single intraperitoneal injection at 30 min before or 10, 30, 60 or 90 min after hypoxia (indicated as *EP or* *). *B*: behavioral assessment; *CCAO*: common carotid artery occlusion; *H*: histological analysis; *W*: western blot analysis. **B**. Quantification of brain tissue loss as a fraction of the total area per section at 7 days after H-I. EP injections were given 30 min prior to H-I at various doses as indicated. **C**. Therapeutic window for EP (50mg/kg). EP injections were given after H-I at the times indicated. **D**. Representative pictures of cresyl violet staining from animals treated with vehicle (H-I) or 50 mg/kg EP (H-I + EP) 10 min after H-I. The upper row shows damage in the frontal cortex and striatum, while the lower row shows cortical and hippocampal damage. **E**. Quantification of tissue loss in cortex, hippocampus and striatum at 7 days after H-I in animals treated with vehicle or EP (50 mg/kg, 10min post-H-I). *p<0.05, **p<0.01 vs. vehicle-treated groups; n=12 animals per group.

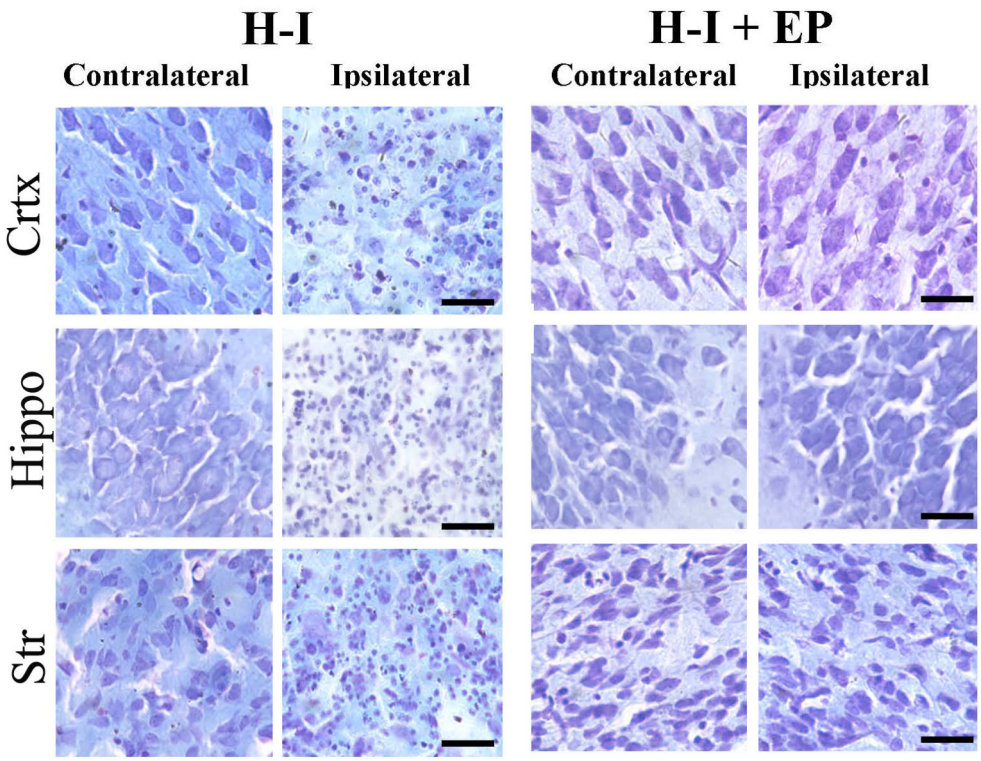

Figure 2. Histological analysis of brain damage in different regions after H-I

Coronal brain sections were obtained from animals treated with vehicle (H-I) or EP (50 mg/kg, 10min post-H-I; H-I + EP) at 7 days after H-I and stained with cresyl violet. Representative pictures of frontal cortex, dorsal hippocampus and striatum from lesioned (ipsilateral) and unlesioned (contralateral) sides are shown. Magnification is 40x (scale bar=30 μm).

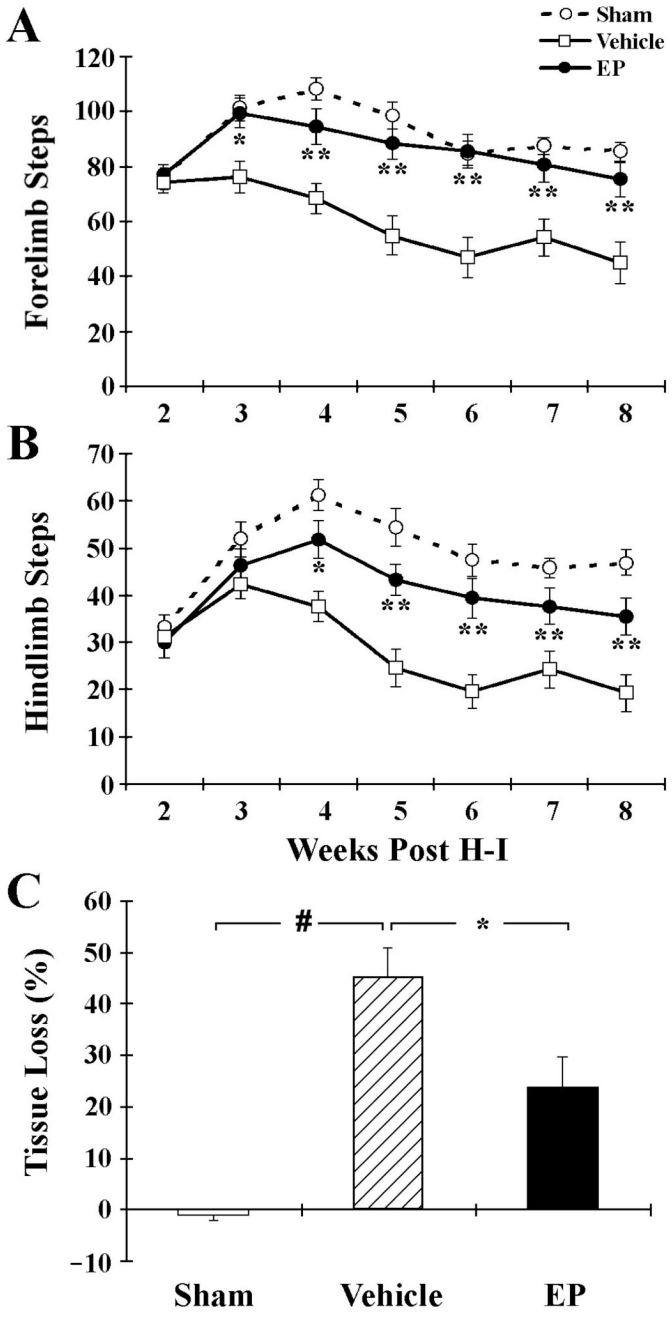

Figure 3. Long-term protection by EP against H-I brain injury

Vehicle or EP (50 mg/kg) was given at 10 min after H-I. **A, B.** Ambulatory behavior was quantified from 2–8 weeks after H-I. Numbers of total forelimb **(A)** and hindlimb **(B)** steps within a 1-min period in the grid-walking test were recorded. n=12–15 animals per group. **C.** Quantification of brain tissue loss at 8 weeks after H-I injury. n=11–12 animals per group. *p<0.05, **p<0.01 vs. vehicle-treated groups; #p<0.01 vs. sham.

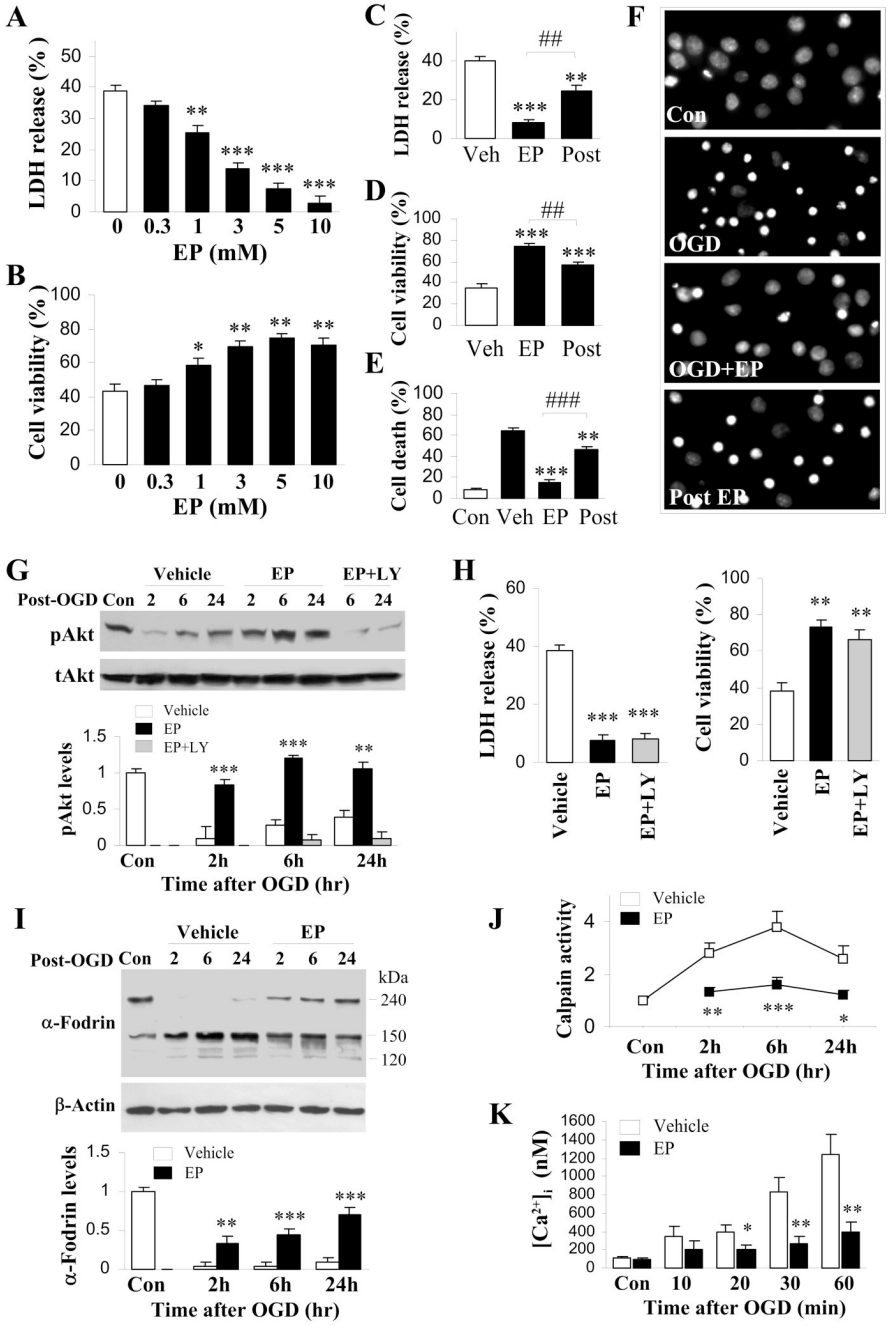

Figure 4. Attenuated cell death and pro-death signaling by EP following *in vitro* ischemia

Cortical neuronal cultures at 12 DIV with EP or vehicle treatment were subjected to 60 min OGD. **A, B.** Cultures were treated with EP (0.3, 1, 3, 5 and 10 mM) or vehicle prior to OGD followed by reperfusion for 24 hr. n=12 from at least three independent experiments. **(A)** Cell death was quantified by measuring LDH release from neurons. Data are expressed as % of total LDH content. **(B)** Cell viability was assessed using Alamar blue. Data are expressed as % of control cells. **C–F.** Cultures were treated with 5 mM EP or vehicle before (EP) or 10 min after (Post) OGD. At 24 hr after OGD, cell death was quantified by measuring LDH release from neurons **(C)** and Hoechst staining (**E**, percentages of condensed/fragmented nuclei; **F**, representative images), while cell viability was assessed using Alamar blue **(D)**. n=12 from at

least three independent experiments. **G, H.** Cultures were pre-treated with vehicle, 5 mM EP with or without LY294002 and subjected to OGD. **(G)** Cell lysates obtained at 2, 6, and 24 hr following OGD were subjected to western blot using phospho-Akt and total Akt specific antibodies. Optical density was quantified by averaging three independent experiments. **(H)** At 24 hr after OGD, cell death was quantified by measuring LDH release from neurons, while cell viability was assessed using Alamar blue. n=12 from at least three independent experiments. **I–K.** Cultures were treated with vehicle or 5 mM EP before OGD, followed by reperfusion of duration as indicated. **(I)** Western blot analysis of α-Fodrin in total protein extract. β-actin was used as loading control. The ratio of densitometry values of α-Fodrin (150 kD band) and β-actin was analyzed and normalized to control. **(J)** Calpain activity was measured in isolated mitochondria. n=3–4 per group. **(K)** Time course of changes of fura-2 AM fluorescence signals. n=3–4 per group. *p<0.05, **p<0.01, ***p<0.001 vs. corresponding vehicle-treated group. # #p<0.01, # # #p<0.001 vs. EP pre-treated OGD group.

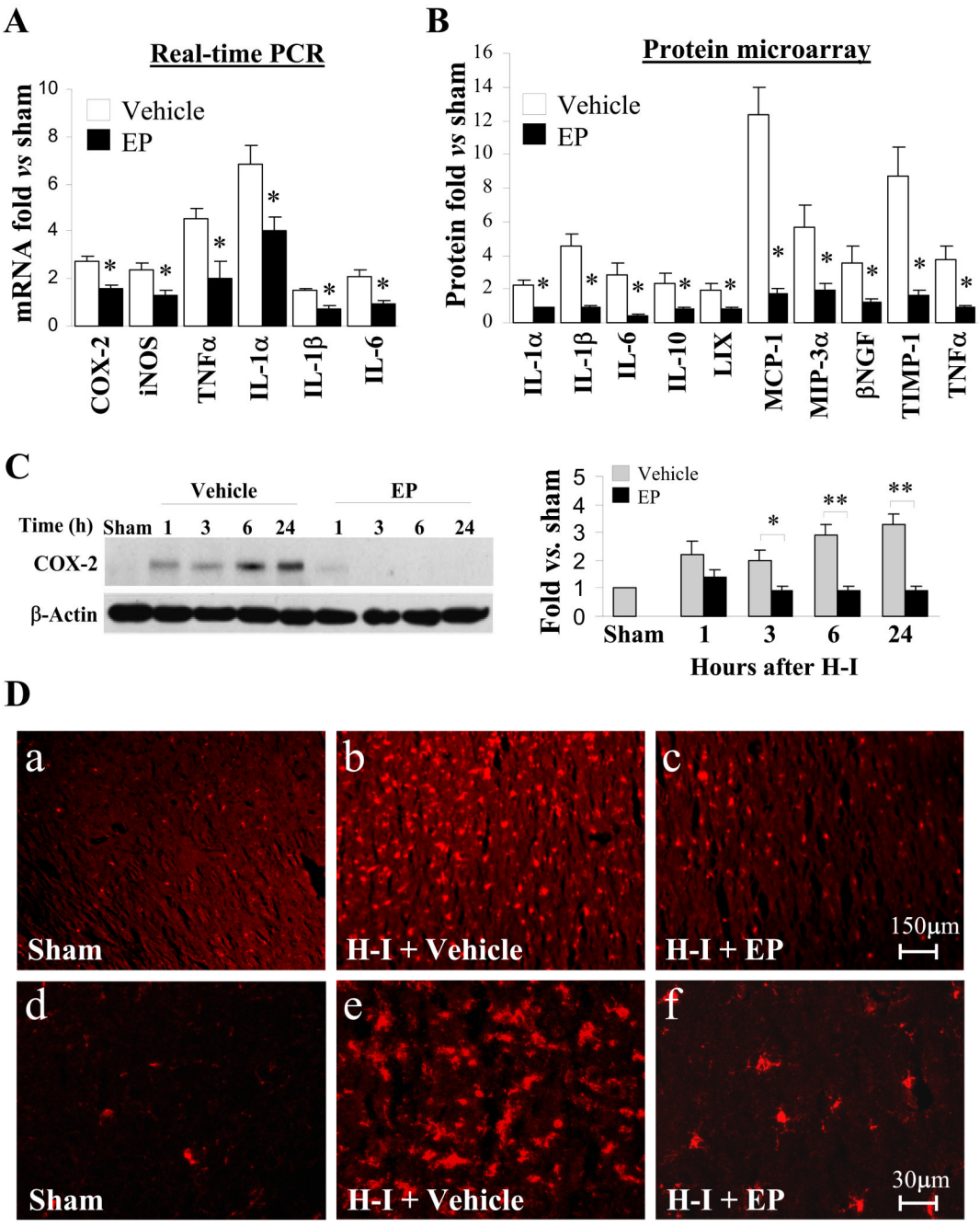

Figure 5. Reduced inflammatory response after H-I in EP-treated P7 pups

Brains were obtained from sham-operated control, vehicle-treated H-I and EP-treated (50 mg/kg, 10min post-H-I) H-I animals. **A.** Real-time RT-PCR analysis in cortical RNA extracts from brains. Data are expressed as fold change versus sham-operated control. n=3 animals per group. **B.** Quantification of proteomic arrays in cortical protein extracts from brains obtained 24 hr after H-I. Data are expressed as fold change versus sham-operated control. n=3 arrays per group. **C.** Western blot analysis of COX-2 in total protein extract obtained at indicated time points after H-I. β-actin was used as loading control. Left panel: representative image of western blot. Right panel: histogram showing the densitometry analysis of COX-2. The ratio of densitometry values of COX-2 and β-actin was analyzed and normalized to each respective

sham-operated control. n=4–6 animals per time point per group. *p<0.05, **p<0.01 vs. corresponding vehicle-treated group. **D.** Representative images of Iba1 staining. The images are representative of three independent experiments.

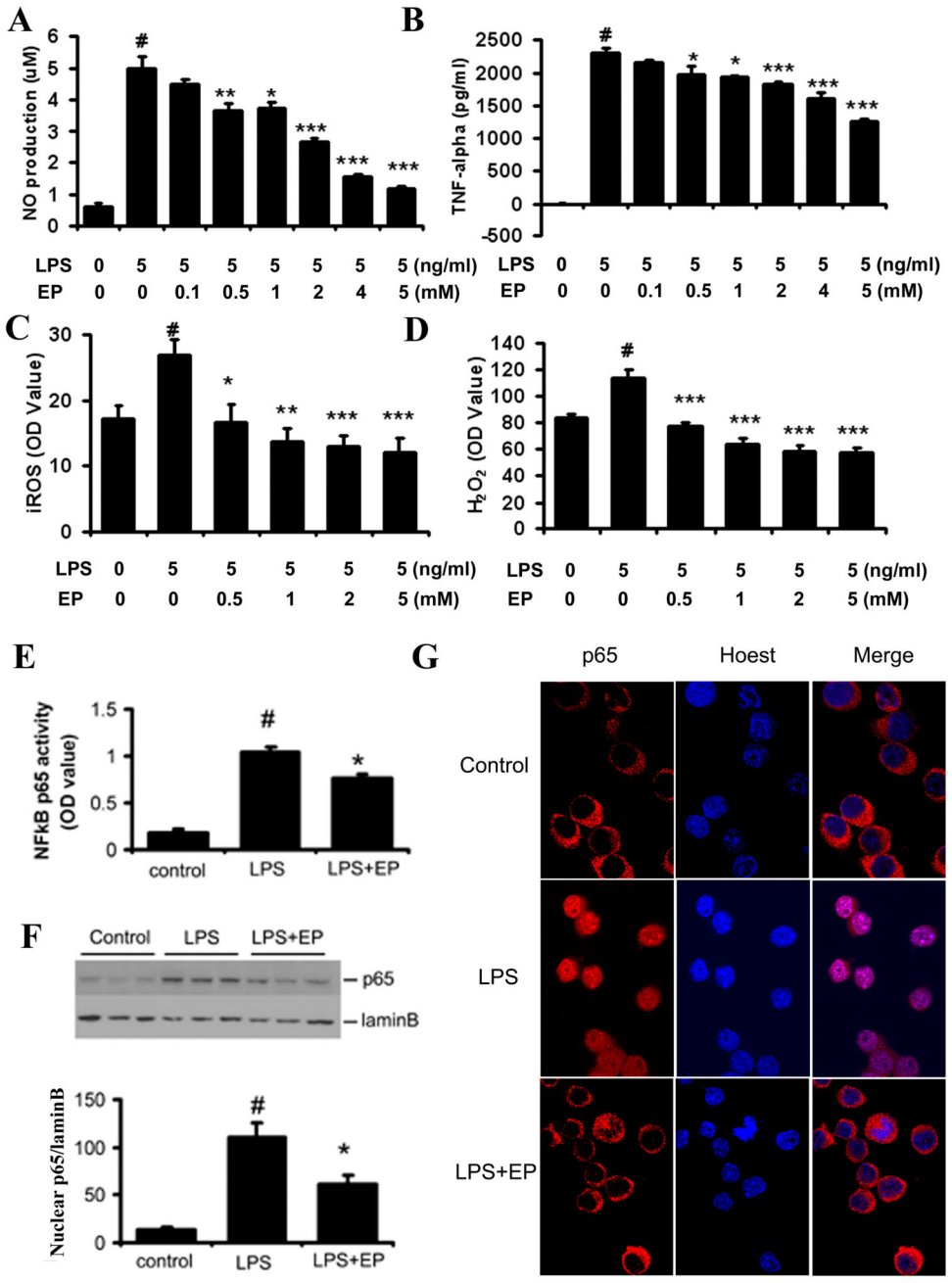

Figure 6. Suppression of LPS-induced activation of HAPI microglial cells by EP

A–D. HAPI microglial cells were treated with different concentrations of EP or vehicle for 1 hr before addition of 100 ng/ml LPS. n=6 in each group. Production of TNF-α **(A)** and nitric oxide (NO) **(B)** was measured 12 hr after LPS. Production of intracellular ROS **(C)** and H_2O_2 **(D)** was measured 45 min after LPS. **E–G.** HAPI microglial cells were treated with 5 mM EP or vehicle for 1 hr and stimulated with 100 ng/ml LPS for 1 hr. Nuclear extracts were prepared. **(E)** NF-κB activity was measured by using the TransAM ELISA assay. **(F)** Expression of nuclear NF-κB/p65 subunit was detected by western blot using a specific antibody. LaminB was used as loading control. Diagram shows quantification of nuclear p65. The ratio of densitometry values of p65 and laminB was analyzed. n=3 in each group. **(G)** LPS-

induced p65 translocation was observed by immunofluorescence in EP- or vehicle-treated HAPI cells. #$p<0.01$ vs. control; *$P<0.05$, **$p<0.01$, ***$p<0.001$ vs. LPS-treated.